Coupling of Neutral-beam-driven Compressional Alfvén Eigenmodes to Kinetic Alfvén Waves in NSTX and Energy Channelling

E. V. Belova[1], N. N. Gorelenkov[1], N. A. Crocker[2], J. B. Lestz[1], E. D. Fredrickson[1], K. Tritz[3]

[1] Princeton Plasma Physics Laboratory, Princeton NJ, USA
[2] University of California, Los Angeles, California, USA
[3] Johns Hopkins University, Baltimore MD, USA

E-mail contact of main author: ebelova@pppl.gov

Abstract. An energy channelling mechanism is proposed to explain flattening of the electron temperature profiles at high beam power in beam-heated National Spherical Torus Experiment (NSTX). High-frequency Alfvén eigenmodes are frequently observed in beam-heated NSTX plasmas, and have been linked to enhanced thermal electron transport and flattening of the electron temperature profiles. Results of 3D nonlinear self-consistent simulations of neutral-beam-driven compressional Alfvén eigenmodes (CAEs) in NSTX are presented that demonstrate strong coupling of CAE to kinetic Alfvén wave at the Alfvén resonance location. It is shown that CAE can channel significant fraction of the beam energy to the location of the resonant mode conversion at the edge of the beam density profile, modifying the energy deposition profile.

1. Introduction

Experimental observations from the National Spherical Torus Experiment (NSTX) suggest that many modes in a sub-cyclotron frequency range are excited during neutral beam injection (NBI). These modes were identified as compressional Alfvén eigenmodes (CAEs) and global Alfvén eigenmodes (GAEs), driven unstable through the Doppler shifted cyclotron resonance with the super Alfvénic NBI ions [1,2]. High-frequency AEs can be excited in ITER due to super Alfvénic velocities and strong anisotropy of the beam ions. They can also be excited by alpha particles near the outer edge of the ITER plasma due to anisotropies in the alpha particle distribution. Observations link GAEs and CAEs to flattening of electron temperature profiles and anomalously low central temperature at high beam power in NSTX [3]. Several mechanisms have been suggested to explain the observed temperature profiles by a strong anomalous electron transport [4]. Other estimates [5] suggest that the energy channeling from core-localized GAEs to continuum damping closer to the edge can be responsible for the observed flattening of the T_e profiles. This paper reports nonlinear MHD-kinetic simulations of NBI-driven CAEs [6], which demonstrate that CAEs can convert to kinetic Alfvén waves (KAW) at the Alfvén resonance location, and thus channel the beam energy to the resonant location at the edge of the beam density profile, modifying the energy deposition profile. It is also shown that strong CAE/KAW coupling follows from the dispersion relation, and will occur for unstable CAEs in other toroidal devices. A set of nonlinear simulations indicate that the CAE instability saturates due to nonlinear particle trapping, and a large fraction of beam energy can be transferred to several unstable CAEs of relatively large amplitudes and absorbed at the resonant location. The absorption rate shows a strong scaling with the beam power.

2. Model

The hybrid code HYM [7] has been used to investigate properties of beam ion driven CAE in NSTX. The HYM code is an initial value 3D nonlinear, global stability code in toroidal geometry, which treats the beam ions using full-orbit, delta-f particle simulations, while the one-fluid resistive MHD model is used to represent the background plasma. In the delta-f method, the equilibrium distribution function of NBI ions $F_0 = F_0(\varepsilon, \lambda, p_\phi)$ needs to be known analytically, and the equation for the perturbed distribution function $\delta F = F - F_0$ is integrated along the particle trajectories. Here ε is the particle energy, $\lambda=\mu B_0/\varepsilon$ is the pitch-angle variable, $p_\varphi = -\psi + R\mathrm{v}_\varphi$ is the normalized toroidal angular momentum, and μ is an adiabatic invariant $\mu=\mu_0+\mu_1$ [7], including first-order and some of the second-order corrections in ρ_i/L (L is the equilibrium magnetic field scale length). The beam ion distribution function is taken to be of the form [7]: $F_0 = F_1(\mathrm{v})F_2(\lambda)F_3(p_\varphi)$, where $\mathrm{v} = \sqrt{2\varepsilon/m_i}$, and functions $F_{1,2,3}$ are defined by

$F_1(\mathrm{v}) = 1/(\mathrm{v}^3 + \mathrm{v}_*^3)$, for $\mathrm{v} < \mathrm{v}_0$,
$F_2(\lambda) = \exp[-(\lambda-\lambda_0)^2/\Delta\lambda^2]$,
$F_3(p_\varphi) = [(p_\varphi - p_{\min})/(p_{\max} - p_{\min})]^\alpha$, for $p_\varphi > p_{\min}$,

where $F_0 = 0$ for $\mathrm{v} > \mathrm{v}_0$ or $p_\varphi < p_{\min}$; v_0 is the injection velocity, and we assumed $\mathrm{v}_* = \mathrm{v}_0/2$. The parameters for the pitch-angle distribution are $\Delta\lambda= 0.3$, and $\lambda_0= 0.7$. The function $F_3(p_\varphi)$ is used to match the experimental profiles of the beam ion density, where $\alpha=6$ is a numerical parameter, and the condition $p_\varphi > p_{\min}$ describes a prompt-loss boundary. A generalized form of the Grad-Shafranov equation solver has been used, which includes, non-perturbatively, the effects of the beam ions with anisotropic distribution [7]. The beam ion beta in the NSTX can be relatively large, and the beam ion current density can be comparable to that of the thermal plasma. As a result, significant modifications of equilibrium occur due to self-consistent inclusion of the beam ions: more peaked current profile, anisotropic total pressure shifted relative to the flux surfaces, and increase in Shafranov shift – which all can have an indirect effect on stability properties.

3. Linear simulation results

The excitation of CAEs has been studied for the H-mode plasma of NSTX shot 141398, where the plasma was heated by 6 MW of 90keV Deuterium beams with $n_b=3.5\times10^{18}$ m^{-3}, $n_e= 6.7\times10^{19}$ m^{-3}, $B_t= 0.325$ T, and $I_p= 0.8$ MA. For this particular shot, normalized beam ion injection velocity was high $V_0/V_A=4.9$ due to a relatively low toroidal field, and as a consequence, significant GAE/CAE activity has been observed. Detailed measurements of GAE and CAE amplitudes and mode structures were obtained [8,9], and the observed modes have been identified as counter-propagating CAE for frequencies f>600 kHz, and small toroidal mode numbers |n|≤5, and as counter-propagating GAEs for f<600 kHz, and |n|~6-8 based on dispersion relations [8]. Co-propagating CAEs with higher toroidal mode numbers n>8 have also been observed in the same shot [9].

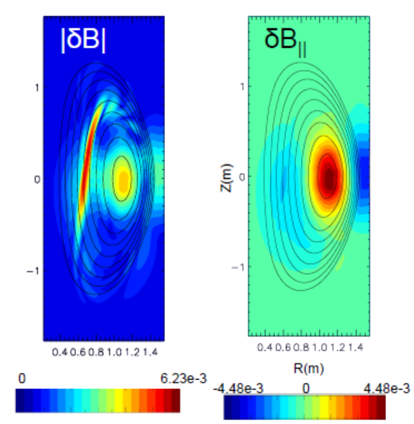

FIG. 1. Contour plots of magnetic field perturbation for n=4 CAE.

Linearized simulations for this case show that the most unstable modes for n=5-7 are counter-rotating GAEs, which have shear Alfvén wave polarization in the core. Most unstable modes for n=4 and n=8, 9 are co-rotating CAEs, driven unstable by the resonant interaction with the beam ions. Calculated frequencies for n=5-7 GAE are ω/ω_{ci}= 0.15 - 0.22 (f= 380-550 kHz), and higher frequencies for CAEs have been obtained with ω/ω_{ci}= 0.35 - 0.5 (f= 870-1200 kHz). Here all frequencies are normalized to the ion cyclotron frequency at the axis f_{ci}= 2.5MHz.

Figure 1 shows poloidal contour plots of the perturbed magnetic field for the n=4 (ω=0.34ω_{ci}) CAE. It can be seen that the CAE is localized in the core, near the magnetic axis, and $\delta B_{||}$ is significantly larger than $\delta B_{\perp}$ everywhere, except in the radially localized region on the high-field-side where the resonant condition ω_A(Z,R)= ω is satisfied (ω_A(Z,R) is the local Alfven frequency, and ω is the frequency of the CAE mode in the simulation). Analysis of magnetic and velocity perturbations of the resonant structure shows that its polarization is consistent with that of the kinetic Alfvén wave (KAW). The numerical model in the HYM code allows a full orbit kinetic description of the beam ions, including the cyclotron resonances, but a one fluid MHD description is used to model the thermal plasma, therefore the radial width of KAW is determined by the beam ion Larmor radius.

The location of the shear Alfvén resonance coincides with the edge of an effective potential well for CAE: $V_{eff} = - \omega^2/V_A^2 + k_{//}^2$, within which the CAE is non-evanescent [2,9], leading to a strong coupling between the compressional mode and KAW. Simulations for both low-n and high-n co-rotating CAEs show resonant coupling to the KAW. Resonance is more pronounced on the HFS, as can be seen, for example, from |δB| plots in Fig. 1. This is related to the shape of the CAE potential well, which is relatively steep on the HFS, and has a very low wall at the LFS. The HYM numerical model treats the thermal plasma as an MHD fluid, and the KAW perpendicular scale in the simulations is determined only by the beam ion FLR effects. Resonance with KAW is located at the edge of the CAE well, and just inside beam ion density profile, and the radial width of the KAW is determined by the beam ion Larmor radius and V_A(R) scale length as $(L\rho^2)^{1/3}$, where ρ is the effective Larmor radius defined by $\rho = \sqrt{3/4\, n_b/n_e}\ \rho_b$ [6]. Inclusion of thermal plasma FLR effects is not expected to change the coupling qualitatively only quantitatively, as follows from the local KAW dispersion relation [6].

Analysis of the particle phase-space for unstable CAEs shows that the resonant particles have a wide range of the pitch-angle parameter λ= 0.1 – 1.2 and energies ε= 10 – 60keV, but a relatively narrow range of resonant $v_{||}$. While this group includes both passing and trapped particles, the analysis shows that co-CAE instability is driven by the trapped ions. A beam ion power scan, described in the next section, allows estimating a damping rate of CAE due to its linear coupling to KAW, and shows that the CAE instability is close to marginal for the experimental parameters. The CAE/KAW coupling is the main linear damping mechanism for CAE, and the damping rate is γ_{damp}= 0.66 γ_{dr} for the n=4 CAE.

4. Nonlinear simulations of n=4 co-CAE

Nonlinear simulations of the n=4 CAE have been performed for the beam ion parameters corresponding to NSTX shot 141398. These simulations have been carried out in order to identify the CAE saturation mechanism, find the mode amplitude at the saturation, and calculate self-consistently the fraction of the beam power going into the excitation of a CAE, being channeled to KAW and absorbed at the resonance. The simulations are fully nonlinear including 32 toroidal harmonics, and show saturation of the n=4 CAE mode. Initial conditions for the nonlinear run were obtained by running the n=4 linearized simulations ($t\omega_{ci}$= 0 - 600, Fig.2) to obtain a converged linear mode structure of the CAE. The nonlinear run starts at $t\omega_{ci}$=600, and also shows growth of the *n*=5, 6, 7 GAEs and *n*=8 CAE modes. The *n*=6 and 7

GAEs have larger linear growth rates than the *n*=4 CAE mode, and saturate at higher amplitudes as seen in Fig.2. The timing of the switch between the n=4 linearized run and the fully nonlinear run was chosen in such a way, as to allow the n=4 CAE saturate ($t\omega_{ci}$~750) while the amplitudes of other unstable modes were still relatively small. This allowed calculation of the fraction of the beam power taken by the n=4 CAE, and calculation of the energy flux from a single CAE to the KAW near the saturation.

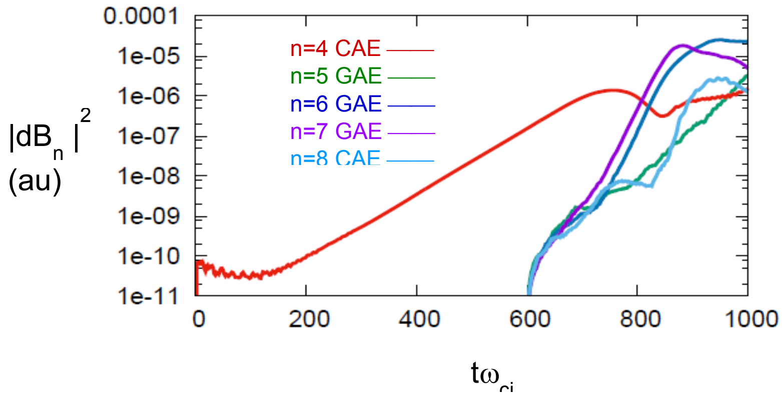

FIG. 2. Time evolution of amplitudes of different toroidal harmonics of the perturbed magnetic field from fully nonlinear simulations of n=4 CAE for NSTX shot 141398.

The saturation amplitude of the n=4 CAE instability in the simulations is $\delta B_{||}/B_0$= 6.6×10^{-3}, which is larger than values obtained by analysing experimental data from the same NSTX shot. Thus, measured plasma displacements of unstable CAEs [8] correspond to magnetic perturbations in the range $\delta B/B_0 \lesssim 3.4\times10^{-3}$, where we have used the HYM-calculated mode structure to relate displacement and magnetic field perturbation amplitudes (more recent calculations suggest even lower experimental values $\delta B/B_0 \lesssim 1\times10^{-3}$ [10]). The instability saturates due to nonlinear particle trapping, which has been confirmed by scaling of the saturation amplitude with the growth rate $\delta B_{||} \sim \gamma^2$, and it has been verified in a separate nonlinear simulation including only the n=4 toroidal harmonic. The rate of change of the beam ion energy, calculated as $dK_{beam}/dt= \int(\boldsymbol{J}_{beam}\boldsymbol{E})\, d^3x$, can be as large as ~1.5MW near the n=4 CAE saturation at $t\sim750(1/\omega_{ci})$, demonstrating that a significant fraction of the total beam power can be transferred to a single CAE of relatively large amplitude. Note that this estimate reduces to ~0.4MW, if scaled to the measured amplitudes of $\delta B/B_0$= 3.4×10^{-3} [6].

Energy flux from unstable CAE to the KAW location can be calculated as $\mathbf{S}=\mathbf{E}\mathrm{x}\mathbf{B}/4\pi + p\mathbf{V}\gamma/(\gamma-1)$, where the bulk plasma kinetic energy flux can be neglected as being a third-order in the perturbation amplitude. Calculations show that the pressure related term has the same sign as the Poynting flux, but it is about 14% of the total flux, proportional to plasma beta. Plots of the energy flux **S** in the poloidal plane (Fig.3) shows that the energy flux is mostly directed radially away from the magnetic axis and towards the HFS resonance with the KAW. There is a significant drop in the energy flux at the KAW location, indicating power absorption. The calculated change of the energy flux across the resonant layer at R= 0.6–0.7 m at time $t=750(1/\omega_{ci})$, corresponding to the peak CAE amplitude, is 3 × 10^5 W/m^2. Estimating the surface area as ~2.4 m^2, the power absorption can be calculated as ~0.7 MW, which is about a half of the rate of change of the beam ion energy. This value might be overestimated, because the numerically obtained CAE saturation amplitude is larger than the observed value. When scaled down to amplitude of $\delta B/B_0$~3.4×10^{-3}, the estimated power absorption becomes ~0.2MW, proportional to the square of the local CAE amplitude. In either case, the nonlinear simulations demonstrate that a significant fraction of the total beam power can go into the excitation of a single CAE, and then be channeled by the CAE to the resonance location at the edge of the beam, and absorbed there. Considering a large number of unstable CAEs observed experimentally in this particular NSTX shot [8], the total power channeled to the KAWs can significantly affect the beam energy deposition profile, and lead to electron heating closer to the edge.

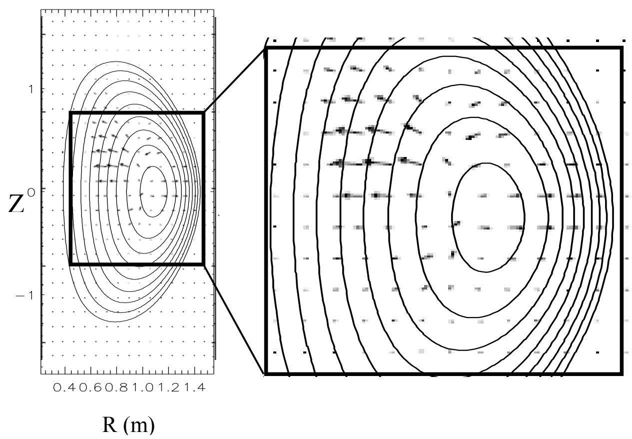

*FIG. 3. Vector plot of the energy flux **S** in poloidal plane from nonlinear simulations of the n=4 CAE/KAW at t=750(1/ω_{ci}).*

An additional set of linearized and nonlinear simulations have been performed for the n=4 CAE instability for varying beam ion density. The results of these simulations, namely the scaling of the instability growth rate, saturation amplitude and mode-converted power are summarized in Fig.4. Simulations have been performed for fixed beam ion distribution function and thermal plasma parameters, except that the peak beam ion density has been varied from $0.03n_e$ to $0.063n_e$. A new self-consistent equilibrium has been calculated for each case. Figure 4a shows that the growth rate of the n=4 CAE scales linearly with beam ion density, and there is a threshold of $n_b \leq 0.035n_e$, below which the mode is stable. The parameters for the NSTX shot #141398 correspond to $n_{b0}=0.053n_e$, and $\gamma=0.0095\omega_{ci}$. Assuming that the instability drive is proportional to the beam ion density and using $0.035n_e$ as threshold density, we can estimate the drive and damping rates from $\gamma= \gamma_{dr} (n_b/n_{b0}) - \gamma_{damp}$, where $\gamma_{damp}= 0.0185\omega_{ci}$ is the CAE damping rate due to coupling to KAW, and $\gamma_{dr}= 0.028\omega_{ci}$ is the beam ion drive for the experimental value of the beam density $n_{b0}=0.053n_e$. Due to strong linear CAE/KAW coupling, the damping rate is large $\gamma_{damp}= 0.66\, \gamma_{dr}$ for the n=4 CAE.

The beam power for the NSTX shot #141398 was P=6MW, therefore the threshold value of the beam power needed for the excitation of the n=4 CAE can be estimated as P~4MW. This estimate is consistent with experimental results showing a large number of unstable subcyclotron frequency Alfven modes when the beam power is sufficiently large P≥4MW [3]. Damping rates of higher-*n* CAEs due to coupling to KAW are expected to be higher than that for small *n*, because of smaller radial extent of the large-n CAE effective potential well, and localization of the resonances at smaller minor radii, where the plasma density is higher and absorption is stronger [11].

Fully nonlinear simulations have been carried out for each value of beam ion density, and show that the saturation amplitude of the n=4 CAE scales approximately as the square of the growth rate, i.e. $|\delta B_{\|}/B_0| \sim (\gamma/\omega_{ci})^2$ (Fig.4b), consistent with the particle trapping saturation mechanism. The absorption rate, calculated as a change in the Poynting flux across the resonance layer, has been obtained in each simulation, and it shows a very strong scaling with growth rate / beam power (Fig.4c). The best fit with the power law gives $\Delta S \sim (\gamma/\omega_{ci})^5$, implying that the energy loss at the resonance scales as a fifth power of the beam ion density (or the beam power). The strong scaling could be explained, if one assumes that the power absorbed at the resonance is proportional to the change in the CAE energy $P = 2\gamma \int (\delta B)^2/4\pi \, d^3x \sim \gamma^5$. These results suggest that the energy channelling mechanism might play a significant role in NSTX-U due to higher projected beam powers, provided that the CAEs are still unstable for larger toroidal field values (i.e. smaller values of v_0/V_A parameter).

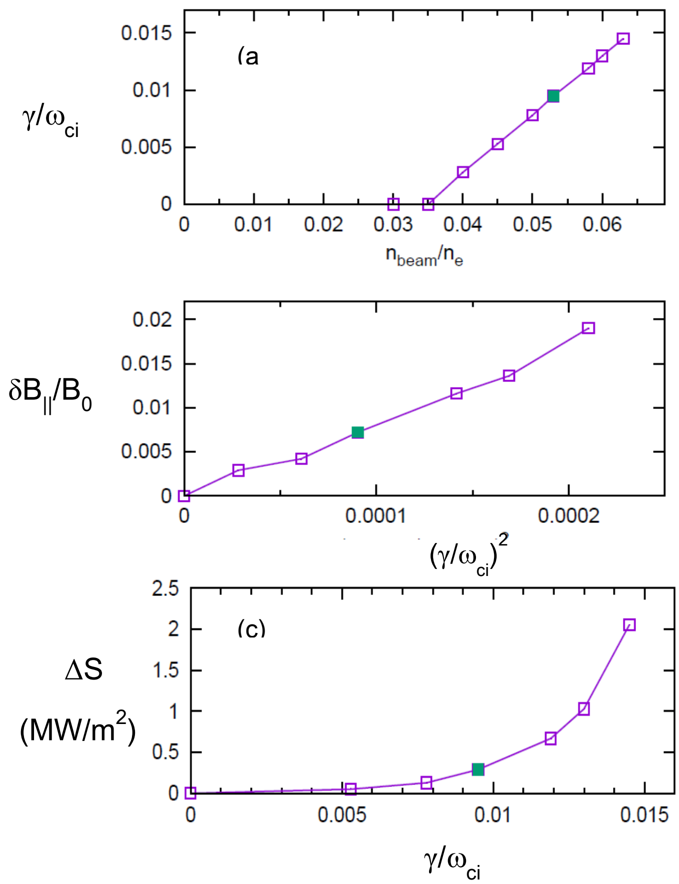

FIG. 4. (a) Dependence of linear growth rate of the n=4 CAE on the beam ion density; (b) Saturation amplitude of CAEs vs square of the linear growth rate; (c) Calculated change of the energy flux at the resonance location near the instability saturation vs the normalized growth rate. Solid symbols (green) correspond to the experimental conditions for NSTX shot #141398.

5. Conclusions

Numerical simulations presented here demonstrate that the beam-driven CAEs are strongly coupled with kinetic Alfven waves at the Alfven resonance location in NSTX. The resonant mode conversion of CAE to KAW occurs for any unstable CAE, independent of toroidal mode number or mode frequency, and it follows from the dispersion relation. The strong linear CAE/KAW coupling supports an alternative mechanism for T_e flattening, in which the beam-driven CAE dissipates its energy at the resonance location close to the edge of the beam, therefore significantly modifying the energy deposition profile (similar to a mechanism suggested qualitatively for GAEs in [5]).

A set of nonlinear simulations demonstrate that the CAE instability saturates due to nonlinear particle trapping, that is, the instability saturates mainly through the changes in the beam ion distribution function, and field nonlinearities play a minor role. The calculated fraction of NBI energy which can be transferred to a single unstable CAE is significant: up to P~0.4MW for one mode with amplitude $\delta B/B_0 \sim 3\cdot 10^{-3}$. Therefore, this study demonstrates that a large fraction of the beam energy can be transferred to several unstable CAEs of relatively large amplitudes and absorbed at the resonant location. Energy flux is shown to be directed away from the magnetic axis (CAE) toward the resonance location (KAW). The absorption rate, calculated as a change in the Poynting flux across the resonance layer, shows a very strong scaling with growth rate (Fig.4c), implying that the energy loss at the resonance scales as a fifth power of the injected beam power. The calculated magnitude of power absorption is significant enough to have a direct effect on the electron temperature profile, provided that the CAE amplitude is sufficiently large $\delta B/B_0 \gtrsim 10^{-3}$.

Strong CAE/KAW coupling follows from the dispersion relation, therefore, the energy channelling mechanism is generic and it applies to any device with unstable CAEs. The CAEs are generally predicted to be unstable in tokamaks with $V_0/V_A>1$ [2], however a recent set of HYM simulations (a parameter scan performed for a fixed shape of the beam ion distribution function) [12] shows that excitation of a significant number of unstable CAEs with different toroidal mode numbers requires relatively large values of normalized beam injection velocity, $V_0/V_A>3$-4. Future work will include investigation of the effects of the details of beam ion distribution function on the CAE and GAE instabilities. A more complete description of the mode conversion in NSTX would require inclusion of the thermal plasma FLR effects, and two-fluid (finite ω/ω_{ci}) effects, which is beyond the scope of this paper.

In summary, it is found that beam-driven CAE modes in NSTX mode-convert to KAWs, and therefore can channel the energy of the beam ions from the injection region near the magnetic axis to the location of the resonant mode conversion at the edge of the beam density profile. This mechanism provides an alternative explanation to the observed reduced heating of the plasma core at high beam power in NSTX. Detailed comparison of the relative importance of the energy channelling and anomalous electron transport mechanisms will be reported in future publication.

6. Acknowledgements

The simulations reported here were carried out using resources of the National Energy Research Scientific Computing Center (NERSC). This research was supported by the U.S. Department of Energy #DE-AC02-09CH11466.

References

[1] E. D. Fredrickson, *et al.*, “Observation of Compressional Alfvén Modes During Neutral-Beam Heating on the National Spherical Torus Experiment,” Phys. Rev. Lett. **87**, 145001 (2001).

[2] N. N. Gorelenkov , E. Fredrickson, E. Belova, et al., “Theory and observations of high frequency Alfvén eigenmodes in low aspect ratio plasmas,” Nucl. Fusion **43**, 228, (2003).

[3] D. Stutman, *et al.*, “Correlation between Electron transport and Shear Alfven Activity in the National Spherical Torus Experiment”, Phys. Rev. Lett. **102**, 115002 (2009).

[4] N.N. Gorelenkov, D. Stutman, K. Tritz et al., "Anomalous electron transport due to multiple high frequency beam ion driven Alfvén eigenmodes"**,** *Nucl. Fusion* **50** 084012 (2010).

[5] Ya. I. Kolesnichenko, Yu. V. Yakovenko, and V. V. Lutsenko, "Channeling of the energy and momentum during energetic-ion-driven instabilities in fusion plasmas", Phys. Rev. Lett., **104**, 075001 (2010).

[6] E. V. Belova, N. N. Gorelenkov, N. A. Crocker, et al., "Coupling of Neutral-beam driven Compressional Alfven Eigenmodes to Kinetic Alfven Waves in NSTX and Energy Channeling", Phys. Rev. Lett., **115**, 015001 (2015).

[7] E. V. Belova, et al., Phys. Plasmas **7**, 4996 (2000); "Self-consistent equilibrium model of low aspect-ratio toroidal plasma with energetic beam ions", **10**, 3240 (2003).

[8] N. A. Crocker, *et al*., "Internal amplitude, structure and identification of compressional and global Alfvén eigenmodes in NSTX," Nucl. Fusion **53**, 043017, (2013).

[9] E. D. Fredrickson, N. N. Gorelenkov, M. Podesta, *et al*., "Non-linear modulation of short wavelength compressional Alfven eigenmodes", Phys. Plasmas, **20**, 042112 (2013).

[10] N. A. Crocker, private communication (2016).

[11] J. A. Heikkinen, T. Hellsten, and M.J. Alava, Fast wave absorption at the Alfven resonance during cyclotron resonance heating, Nucl. Fusion **31**, 417 (1991).

[12] J. Lestz, E.V. Belova, N.N. Gorelenkov, Hybrid MHD/particle simulation study of subcyclotron Alfven eigenmodes in NSTX, Bull. Am. Phys. Soc. **60**, 146 (2015).